Peer-reviewed version available at Metals 2017, 7, 457; doi:10.3390/met7110457

Article

Study of the influence of TiB content and temperature in the properties of in situ titanium matrix composites

Cristina Arévalo[1], Isabel Montealegre-Melendez[1,*], Eva M. Pérez-Soriano[1], Enrique Ariza[2], Michael Kitzmantel[2] and Erich Neubauer[2]

[1] Department of Engineering and Materials Science and Transportation, School of Engineering, University of Seville, Camino de los Descubrimientos s/n, 41092, Seville, Spain; carevalo@us.es (I.M.); evamps@us.es (E.M.P.-S.)

[2] RHP-Technology GmbH, Forschungs- und Technologiezentrum, 2444 Seibersdorf, Austria; enrarigal1@hotmail.com (E.A.); michael.kitzmantel@rhp-technology.com (M.K.); erich.neubauer@rhp-technology.com (E.N.);

* Correspondence: imontealegre@us.es (C.A.); Tel.: +34-954-482-278

Abstract: This work focuses on the study of the microstructure, hardening and stiffening effect caused by the secondary phases formed in titanium matrices. These secondary phases were originated from reactions between the matrix and boron particles added in the starting mixtures of the composites. Not only was the composite composition studied as an influencing factor in the behaviour of the composites, but also different operational temperatures. Three volume percentages of boron content were tested (0.9, 2.5 and 5 vol % of amorphous boron). The manufacturing process used to produce the composites was inductive hot pressing, which operational temperatures were between 1000 °C to 1300 °C. Specimens showed optimal densification. Moreover, microstructural study revealed the formation of TiB in various shapes and proportions. Mechanical testing confirmed that the secondary phases had a positive influence on the properties of the composites. In general, adding boron particles increased the hardness and stiffness of the composites; however rising temperatures resulted in greater increases in stiffness than in hardness.

Keywords: in situ Titanium composites, microstructure analysis, TiB precipitates

1. Introduction

Over the last few decades, titanium matrix composites (TMCs) have been considered as valuable materials for diverse applications in the aerospace industry. The sector demands materials that can achieve high specific stiffness in addition to possessing good thermal stability at high operational temperature, such as TMCs [1, 2]. Regarding the diverse methods used to develop these materials, synthesizing in situ is currently considered one of the best techniques due to the excellent properties of the produced materials. The main advantage of these kinds of composites lies in the stable interface formed between the matrix and the reinforcing phase [3]. The high reactivity of the titanium with several ceramic compounds provides a wide range of options for selecting the elemental materials to manufacture in situ TMCs [4-9]. Among the diverse materials that could act as reactive compounds with titanium, boron (B) has been considered as a suitable candidate to start in situ secondary reinforcing phases. Many recent works have presented this non-metallic element as an ideal reactive to promote the formation of TiB and TiB_2. The significance of these borides as reinforcements is based on the fact that they are chemically compatible with the matrix, in addition to having similar densities and thermal expansion coefficients [10-12].

With regards to TMC manufacturing processes, powder metallurgy (PM) has been shown in many studies to be the most suitable when compared to traditional processes [2]. PM technologies overcome certain problems of conventional processes: wettability between the matrix and the ceramic reinforcements, and long and complex processing steps [13]. In particular, inductive hot processing (iHP) technology is valued for TMCs manufacturing due to its short operational time. The use of this technique has facilitated the investigation of TMCs' properties and the secondary phases formed at different processing temperatures [14, 15]. Despite the advantages of this process, the restrictions of the specimens' size (diameters of 20 mm) limit the measurement of tensile and bending properties of the final specimens. For that reason, in this work, in addition to the iHP process, Direct Hot Pressing (dHP) technology has been employed.

The scope of this research is the study and evaluation of the relationship between the compositions of determinate TMCs, their processing conditions and their final properties.

2. Materials and experimental procedures

The starting materials were commercial Ti powders grade 1 and amorphous B particles, manufactured by TLS GmbH (Germany) and ABCR GmbH & Co. KG (Germany) respectively. The characterisation of both powders was performed to verify the information about their size and morphology supplied by the manufacturers. The particle size distribution of the starting powders was determined by laser diffraction analysis (Mastersizer 2000). The average particle size of the titanium and amorphous boron powders are listed in Table 1.

Table 1. Particle size distributions of the starting powders.

	Ti [μm]	Amorphous B [μm]
D10	11.88	0.74
D50	28.13	2.44
D90	51.42	14.51

Before the hot consolidation of the composites, the blends of the powders were prepared. The tested compositions and their operational parameters are shown in Table 2. The titanium powder and each different volume percentage (vol %) of the amorphous B particles were mixed by tubular machine (Sintrix) for 16 hours with ceramic balls (ZrO_2) of 3 mm diameter. The weight ratio of ceramic balls to powder was 10:1. Moreover, the use of hexane helped towards the distribution of the fine particles of amorphous B in the metallic matrix. The powder mixture was dried and subsequently blended a second time for several minutes without the ceramic balls, to avoid possible agglomerations. This was the same blending procedure used for producing composites as in previous authors' works [15, 16]. Then, the target composition of three different powder mixtures was made from titanium and 0.9 vol %, 2.5 vol % and 5 vol % of B particles. With these compositions the predesigned values of TiB are 2.65 vol %, 7.42 vol % and 15.02 vol % respectively. These values were calculated based on the theoretical densities: i) 4.51 g/cm^3 for titanium, ii) 4.56 g/cm^3 for TiB, and iii) 2.46 g/cm^3 for boron [1].

Subsequently, the hot and rapid consolidation of the specimens was carried out. Two machines were employed to manufacture the specimens. The first was a self-made hot pressing machine, inductive Hot Pressing (iHP) equipment made by RHP-Technology GmbH & Co. KG. Its main advantage is its high heating rate due to its special inductive heating set-up. The die used for all the iHP cycles was made from graphite (punch Ø 20 mm). It was lined with thin paper with a protective coating of boron nitride (BN) for each iHP cycle. Six specimens were consolidated by this iHP method (see Table 2). The second machine was used to fabricate specimens with suitable dimensions in order to measure their mechanical properties. Assuming the composite with low properties and TiB precipitates formation (5 vol % B at 1000 °C), a second rapid hot pressing machine (direct hot pressing dHP with larger die (Ø 80 mm)) was also used in order to measure mechanical properties.

Table 2. Composition and processing parameters for the manufacturing of TMCs.

Amorphous B [vol %]	Temperature [°C]	Pressure [MPa]	Dwell time [min]	Processing method	Diameter [mm]
0.9	1100	50	15	iHP	20
2.5	1100	50	15	iHP	20
5	1000	50	15	iHP	20
5	1000	35	15	dHP	80
5	1100	50	15	iHP	20
5	1200	50	15	iHP	20
5	1300	50	15	iHP	20

* inductive Hot Pressing (iHP) and direct Hot Pressing (dHP)

Regarding the operational parameters, Figure 1 shows the evolution of cycle's parameters for each of the composites' manufacturing runs in terms of temperature, pressure and displacement of the punches (uniaxial press). Figure 1 a) relates to the representative cycle in each of the hot pressing machines. For dHP, the starting pressure and the heating rate are lower than in iHP due to requirements of this technique.

The graphs shown in Figure 1 b) are drawn in a quantitative way in order to compare all the run cycles across both iHP and dHP equipments. As it is appreciated, the temperature versus time is represented in addition to the punch displacement versus time. In all the cycles, the holding time (15 min) and the vacuum conditions (10^{-5} bar) were fixed. In particular for the iHP runs, the consolidation temperature was varied: 1000 °C, 1100 °C, 1200 °C and 1300 °C (see in Figure 1 b)). These values of temperature were employed to investigate the effect of 100 °C increments in the microstructure and properties of specimens made from same starting powder composition. In case of the specimen fabricated by dHP, the operational conditions were similar than the iHP ones; however, only an operational temperature of 1000 °C was set. This value was fixed according to a previous authors' work in which an interesting microstructure phenomenon took place at this temperature in TMCs at similar conditions, but made from different raw materials [15].

Once the iHP and dHP cycles were finished, the samples with 20 mm and 80 mm of diameter were taken out from the respective dies and cleaned by a sand blasting machine to remove the graphite paper remains from the surfaces. Then, the characterization of all the specimens was performed. Firstly, metallographic preparation of all the specimens was carried out carefully to study the newly-formed phases and the microstructure of the TMCs. Then, X-ray diffraction (XRD) equipment (Brunker D8 Advance A25) was employed to identify the diverse crystalline phases in the composites. The microstructure characterisation was studied by optical microscope (OM), Nikon Model Epiphot 200 equipment, and by scanning electron microscope (SEM) JEOL 6460LV, integrated with electron backscatter diffraction (EBSD) detector and Energy Dispersive Spectroscopy (EDS). The measurements of the precipitates' sizes were performed using the software Image-Pro Plus 6.2.

Preprints (www.preprints.org) | NOT PEER-REVIEWED | Posted: 27 September 2017 doi:10.20944/preprints201709.0140.v1

Peer-reviewed version available at Metals 2017, 7, 457; doi:10.3390/met7110457

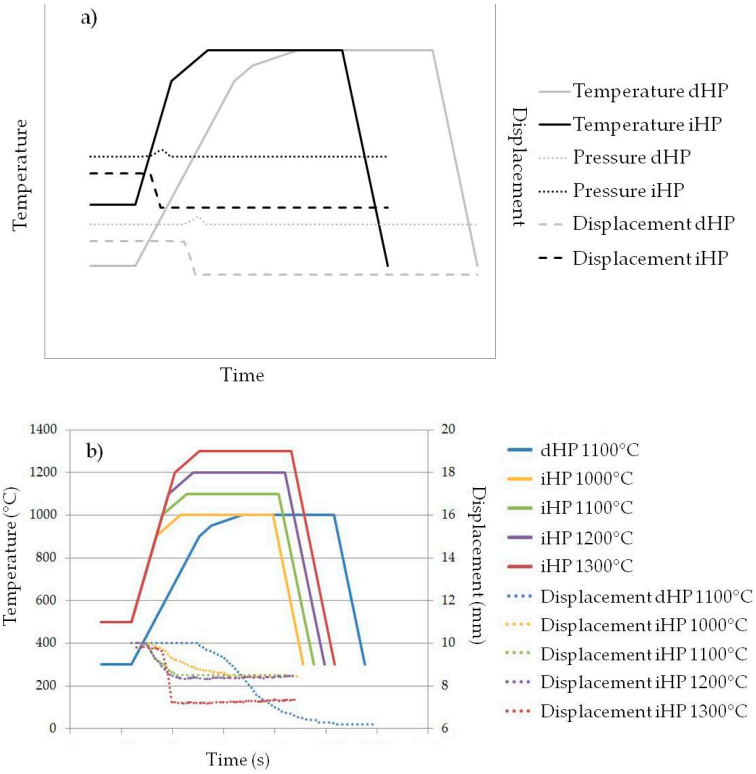

Figure 1. a) Graphical representation of temperature vs. time in iHP and dHP cycles; b) temperature variations vs. time and shrinkage displacements vs. time for TMCs processing cycles from the same starting powders.

The density of the specimens was measured by Archimedes' method (ASTM C373-14). The results were compared to the theoretical density calculated by rule of mixtures. Hardness measurements were carried out on the polished cross-sections of the specimens. Eight indentations were done by a tester model, Struers-Duramin A300, to ascertain the Vickers hardness (HV10). The estimation of the specimens' Young's Modulus was made by ultrasonic method (Olympus 38 DL). It was used with a pulse generator/receiver, recording the transit time (outward/return) through the thickness. This technique allowed the determination of both the longitudinal (VL) and transverse (VT) propagation velocities of acoustic waves. To correctly measure the propagation velocities of these waves, the surface of samples must be properly grinded and polished (to create samples with smooth and parallel surfaces) and the delay times of transducers minimised by following an iterative measurement protocol. The Young's Modulus was calculated from the density (g/cm^3), VL and VT [17]. Tensile tests were performed on a universal testing machine Instron 5505 with a strain rate of 1 mm/min. Additionally, the same machine was employed to carry out the flexural tests at 5 mm/min. Both properties were evaluated according to the standards UNE EN 10002-1:2002 and UNE EN ISO3325 respectively.

3. Results and discussion

The obtained results are presented and discussed considering the two main issues of this work: i) the influence of starting powder compositions (vol % of amorphous B) at identical processing conditions, ii) the effect of rising temperature (1000 °C, 1100 °C, 1200 °C and 1300 °C) for the same starting powder mixture (5 vol % of amorphous B).

3.1. Microstructural study and XRD analysis

Firstly, taking into account the volume percentages (vol %) of the amorphous B particles added in the blend, the microstructures of the specimens are compared. Figure 2 shows the SEM images of three specimens fabricated at 1100 °C for 15 minutes and made from the mixtures of Ti and amorphous B

Peer-reviewed version available at Metals 2017, 7, 457; doi:10.3390/met7110457

with 0.9 vol %, 2.5 vol % and 5 vol %, respectively. As it might be expected, precipitates are observed in the microstructure of the specimens, since at this temperature (1100 °C) there have been reactions between the matrix and the boron particles [3, 18]. As many authors have previously described, these precipitates are supposed to be in situ formed TiB [15, 19] because of this reaction (see Figure 2). It is important to highlight a clear evolution of the size and the volume of the precipitates related to the amorphous B content (vol %). As predicted, the increment of the B content in the composites causes the apparition of more borides precipitates.

Two different morphologies of TiB precipitates can be appreciated: whiskers and rounded hexagonal shapes (Figure 2). To verify the composition of both types of precipitates, EDS analysis has been performed in the marked spots in Figure 2 b). Using 0.9 vol % of B particles, the size of the round precipitates is the smallest one compared to the rest of the precipitates' size formed in TMCs, with B contents of 2.5 vol % and 5 vol %. It is observed that increasing the content of B, the size of the precipitates also increased. The whiskers' lengths remain generally constant although the widths increase slightly by increasing the B content. Moreover, the round hexagonal precipitates become larger. In Figure 2 c) there are some darker grey areas where the B particles remain in the titanium matrix without reacting.

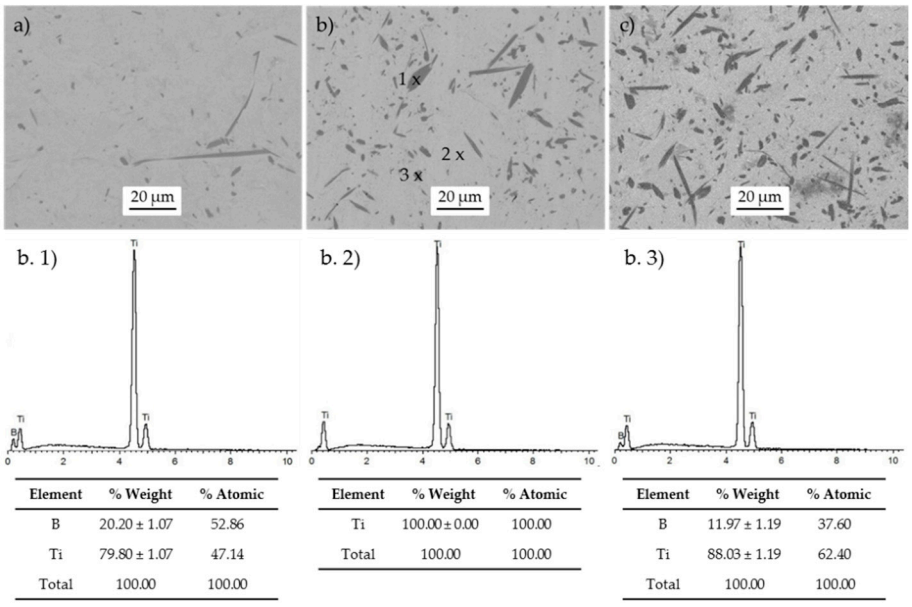

Element	% Weight	% Atomic
B	20.20 ± 1.07	52.86
Ti	79.80 ± 1.07	47.14
Total	100.00	100.00

Element	% Weight	% Atomic
Ti	100.00 ± 0.00	100.00
Total	100.00	100.00

Element	% Weight	% Atomic
B	11.97 ± 1.19	37.60
Ti	88.03 ± 1.19	62.40
Total	100.00	100.00

Figure 2. SEM images of TMCs manufactured at 1100 °C with different content of amorphous B in their starting powders: a) 0.9 vol %; b) 2.5 vol % (EDS spectra spot 1), spot 2) and spot 3)); and 5 vol %.

The second target parameter of the study is the processing temperature for specimens fabricated from identical starting powder (5 vol % of amorphous B). There are relevant changes in the microstructures of the composites caused by increasing the consolidation temperature from 1000 °C to 1300 °C. This phenomenon can be observed in Figure 3. The lower the temperature, the fewer the number of formed precipitates. Titanium grains can be clearly recognised (see spot 2 in Figure 3 a)). Additionally, there are possible agglomerations of the reinforcing phases located in these grain boundaries. Regarding the reaction between Ti and B at 1000 °C, the time (15 min) and operational temperature are insufficient to promote an atomic diffusion phenomenon of boron into the matrix grains. EDS analysis reveals grey areas corresponding to such B particles agglomeration (see in Figure 3). However, only one increment of 100 °C (from 1000 °C to 1100 °C) causes the origin of TiB precipitates in the matrix with the two different morphologies previously mentioned. When the operational temperature rises from 1100°C to 1200°C, the size of the round hexagonal shapes becomes

Peer-reviewed version available at Metals 2017, 7, 457; doi:10.3390/met7110457

bigger (see Figure 3 b) and c)). In relation to the whisker morphology, the changes caused by the increment of the temperature are more easily appreciated in their thickness than in their length.

The tendency to thicken the size of the precipitates remains constant up to 1200 °C. Comparing the microstructure of Figure 3 c) and Figure 3 d), variations in size of the precipitates are not visible. In both SEM images (TMCs fabricated at 1200 °C and 1300 °C) the thickness of the whiskers are larger than the ones formed at 1100 °C. However, the size of the round hexagonal precipitates is a little bigger than in TMCs processes at 1100 °C.

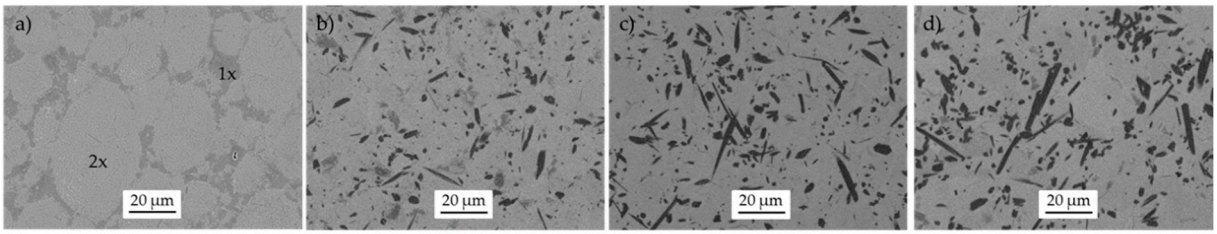

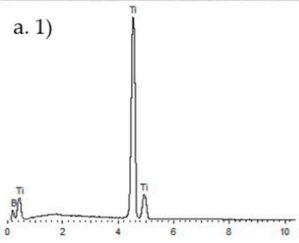

Element	% Weight	% Atomic
B	18.65 ± 0.94	50.39
Ti	81.35 ± 0.94	49.61
Total	100.00	100.00

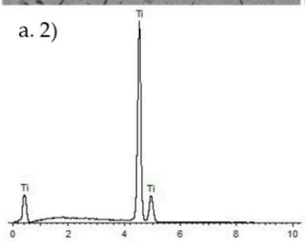

Element	% Weight	% Atomic
Ti	100.00 ± 0.00	100.00
Total	100.00	100.00

Figure 3. SEM images of TMCs made from starting powder with 5 vol % of amorphous B and manufactured at: a) 1000 °C; b) 1100 °C; c) 1200 °C; and d) 1300 °C.

To go into detail about precipitates, a semi-quantitative study of both types of precipitates (whiskers and round shapes), considering their size and frequency/image, were developed by image analysis (using ten SEM images at the same magnifications for each specimen). It is important to note that, in the specimens where their precipitates are located at the grain boundaries, this image analysis could not be carried out. The main parameters evaluated after the image analysis are: i) mean length and mean width of the whiskers, ii) maximum length and maximum width of the whiskers and iii) mean and maximum diameter for the round shapes precipitates. The results of the measurements are represented in Figure 4.

In general, there are more whisker precipitates than round shapes independently of the composite compositions and processing temperature.

Concerning the dimensions of the whisker precipitates, the increase of the temperature and the boron content in the starting blend involves an increase of both mean values (length and width). Figure 4 c) shows a gradual growth in whisker size at higher temperatures and at higher volumes of boron. Each increment of 100 °C drives the growth of whisker mean length size by approximately 15% at the same composite composition. However, the effect of the processing temperature and the boron addition is not the same in the maximum length and width of the whiskers. Despite increasing both temperature and composition, a dimensional limit around 26 µm exists in their maximum length. This means that there are not whiskers measured with length higher than 26 µm independently of these two factors. Regarding the maximum width, it is affected only by temperature, maintains a value of around 0.12 µm across different compositions

With respect to the round-shaped precipitates (Figure 4 d)), the higher the temperature and the volume of boron content are, the higher mean and maximum diameters of the precipitates. An

increment of 100 °C, from 1100 °C to 1200 °C, produces a 21% increase to the mean diameters of these precipitates.

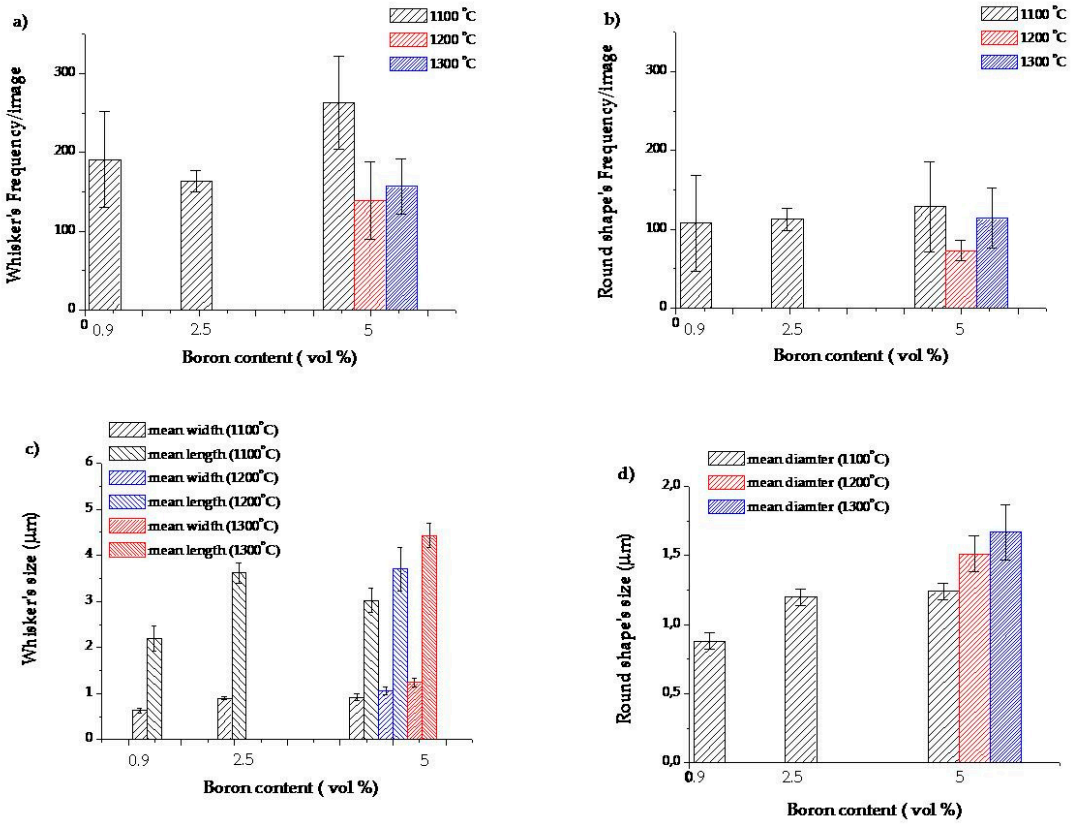

Figure 4. a) Whisker frequency and b) Round shape precipitate frequency vs. Boron content, c) Whiskers size and d) Round shape precipitate size vs. Boron content.

Related to the manufacturing processes, iHP and dHP, similar microstructures of composites were observed in specimens from the same starting powder in spite of their different fabrication methods. This means that at the same processing conditions (1000 °C for 15 min) but in different hot pressing machines, the microstructural properties are alike (see Figure 5). It could therefore be argued that the results obtained could be reproduced using either machine. At 1000 °C, there is insufficient diffusion time and temperature to end the boron source to form TiB.

The phenomenon of the agglomeration of B particles at the grain boundaries and inhomogeneous microstructure was observed in both composites.

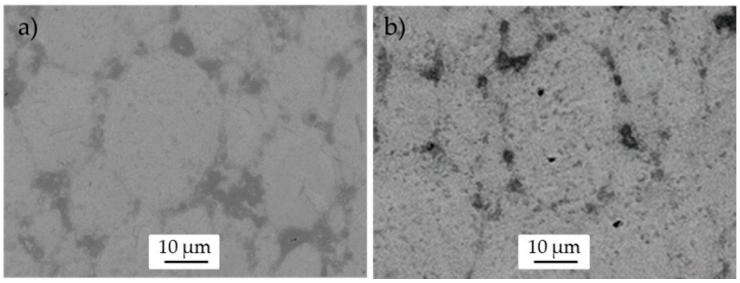

Figure 5. SEM images of TMCs made from starting powder with 5 vol % of amorphous B at 1000 °C for 15 min via a) iHP; b) dHP.

The results of XRD analyses confirm the TiB formation as a product of the reaction between the matrix and the B particles. Figure 6 and Figure 7 show the XRD patterns of the composites made from several starting powders (vol % of B) and processing at different temperatures, respectively. In general, no recordable peaks of TiB_2 are observed in all of the XRD patterns. Comparing the effect of the starting powder compositions, the lower the B content is, the lower the observed peak of TiB is (see Figure 6 a)). However, at the same operational conditions, increasing the vol % of B to 5 %, there are sharper peaks for TiB phase (see in Figure 6 c)). The influence of temperature on the formation of the TiB phase is quite clear as shown by the XRD patterns in Figure 7. It is well known that, by increasing temperature, the reaction between Ti and B tends to be more complete. This can be seen clearly in Figure 7. XRD peaks of TiB in composite produced at 1000 °C are slightly weaker than the ones in the pattern of composite produced at 1100 °C. Moreover, there are two new weak peaks corresponding to the TiB phase when the temperature increases from 1100 °C to 1200 °C.

However, there is not significant variation in the pattern of composites processed at 1300 °C compared to specimens produced at 1200 °C. This is in agreement with the results of the microstructural analysis described previously. The reason is related to the diffusion phenomena in both cases being high enough (at 1200°C and 1300 °C). At these high temperatures, the content of TiB could be higher if the time were to be increased.

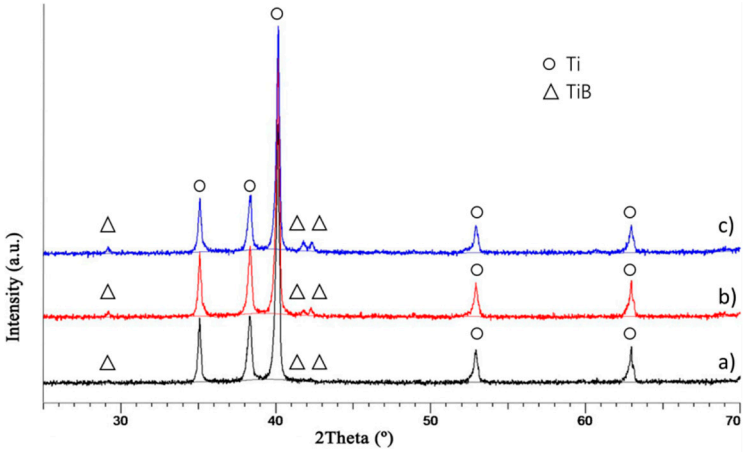

Figure 6. XRD patterns of composites manufacture at 1100 °C for 15 min via iHP with different % vol of B: a) 0.9 vol %; b) 2.5 vol %; and c) 5 vol %.

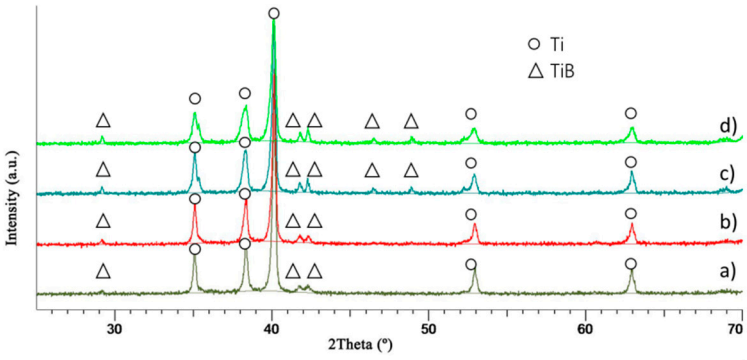

Figure 7. XRD patterns of composites manufacture with 5 vol % of B for 15 min via iHP at different temperatures: a) 1000 °C; b) 1100 °C; c) 1200 °C; and d) 1300 °C.

The semi-quantitative analyses, made by Reference Intensity Ratio (RIR) method, allowed the determination of TiB fractions (see Figure 8). The calculated values of TiB (vol %) are lower than the theoretical values of in situ formed TiB (considering full reaction between the matrix and the B particles). The incomplete reaction between the Ti and B could be the responsible of such differences.

The higher the B content, the greater the differences are between the in situ formed TiB at 1100 °C and the TiB content calculated theoretically. Increasing the temperature from 1000°C to 1100°C leads to a slight increase of the amount of TiB formed. However, when the temperatures reach 1200 °C and 1300 °C there are fewer differences between the in situ formed TiB and the theoretical one.

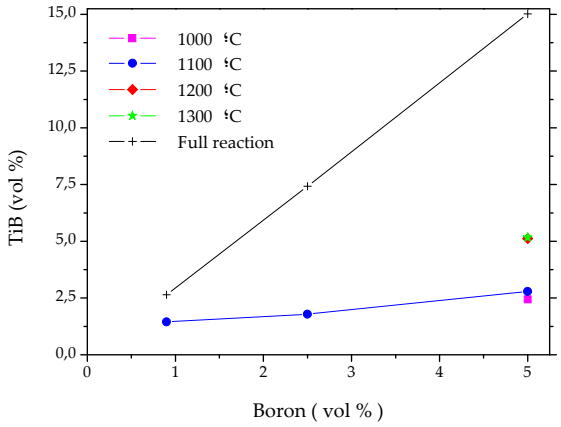

Figure 8. Volume percentage of TiB formed by full reaction Ti-B vs volume percentage of Boron added as starting material.

3. 2 Density, Hardness, Young's Modulus and Mechanical properties

In general, the relative density of the TMCs reaches values of 98%. There is an improving effect in the densification resulting from the increase of the processing temperature. The hardening and stiffening effects induced by the TiB precipitates, in addition to the grain refinement due to the reinforcement content, are two phenomena described by previous authors [13, 18]. Both phenomena are also observed in the in situ TMCs fabricated from the three powder mixtures (0.9 %, 2.5 % and 5% vol of Boron) and at different temperatures (1000 °C, 1100 °C, 1200 °C and 1300 °C). On one hand, as shown in Figure 9 a), the higher the B content the higher the hardness and the Young's Modulus. The hardness increases by 5 % from 0.9 vol % to 2.5 vol % B content and by 32 % from 0.9 vol % to 5 vol %. This is closely related to the in situ formed TiB as shown in Figure 8. Clearly, the content of the reinforcement particles and secondary phases contribute to the hardening effect. The tendency of the Young's Modulus to increase is less pronounced than the hardness' trend with values of 5% and 18% respectively (see in Figure 9 a)).

On the other hand, the increasing the temperature also promotes the variations in the hardness and Young' Modulus due to the number of precipitates. In this case, the increase of the temperature more greatly affects the enhancement of the Young's Modulus than the hardness of the specimens. In general, the values of the hardness remain around 300 HV while the Young's modulus values present increase related to the specimens processed at 1000 °C; 4 %, 10% and 25 % for 1100 °C, 1200 °C and 1300 °C respectively (see Figure 9 b)). Even although the microstructure seems similar in specimens produced at 1200 °C and 1300 °C, the increase of stiffness could be the result of ongoing reactions in the matrix.

Preprints (www.preprints.org) | NOT PEER-REVIEWED | Posted: 27 September 2017 doi:10.20944/preprints201709.0140.v1

Peer-reviewed version available at Metals 2017, 7, 457; doi:10.3390/met7110457

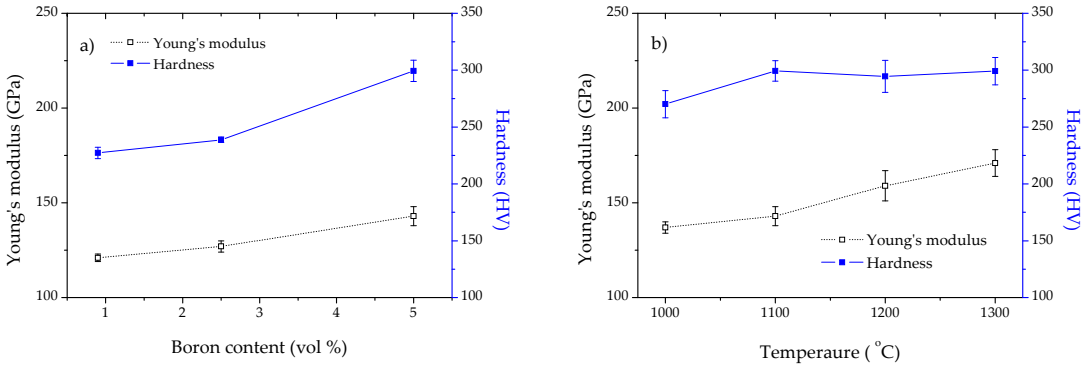

Figure 9. Hardness and Young's Modulus vs.: a) volume percentage of Boron (vol %), b) operational temperatures.

To study the specimen's microstructure and its mechanical behaviour, the composite produced from the powder mixture with 5 % of volume percentage of boron and hot pressed at 1000 °C was also fabricated via dHP to carry out tensile and bending tests. Table 3 shows a summary of the tensile properties tested at room temperature and at 250 °C; additionally, the flexural behaviour of this kind of composite is also presented.

Table 3. Mechanical properties of in situ TMCs produced at 1000 °C with 5 vol % of Boron.

Material	Tensile properties				Bending properties	
	Room temperature		250 °C		Room temperature	
Ti + 5 % vol. of B	σ_{UTS} [MPa]	ε [%]	σ_{UTS} [MPa]	ε [%]	σ_{UBS} [MPa]	ε [%]
	780	1.94	533	6.18	1454.38	3.44

With respect to the tensile properties measured at room temperature, there is an increase in the σ_{UTS} (MPa) due to the boron addition (values are compared to the σ_{UTS} of pure Ti grade 1 [20,21]). However, the ductility behaviour is significantly lower compared to the reference values of pure Ti grade 1 (20%). The distribution of the reinforcement in the matrix and the in situ formed TiB increase the strength of the material. The location of the reinforcement of some particles around the matrix grains blocks the dislocation motion promoting the embrittlement of the matrix and improving the strength of the material. When the tensile test is carried out at 250 °C, there is an increase in the percentage of the maximum deformation of the material. However, the σ_{UTS} measured at this temperature shows a lower value than σ_{UTS} measured at room temperature. As expected, the motion of the dislocation was encouraged by the increase of the temperature during the tensile test. There is a considerable enhancement to the σ_{UBS}.

From a point of view of the microstructural behaviour, specimens in which the distribution of precipitates is homogenous inside the matrix, better mechanical behaviour can be expected with respect to density, hardness and Young's Modulus.

5. Conclusions

The following conclusions can be drawn:

- High densification composites are produced. The influence of the in situ formed TiB and processing conditions on the material behaviour is verified

- The microstructural study reveals changes in the composites depending on the operational temperatures. In the range of 1000 °C to 1100 °C, the location of the precipitates and the boron

particles evolves from the grain boundaries into the matrix. Up to 1100 °C, two different morphologies of TiB precipitates originate: whiskers and round shapes. Increasing the temperature promotes a gradual growth of the TiB phases. At the same composite composition, the TiB precipitates remained relatively constant even if the temperature rose from 1200 °C to 1300 °C.

- Relating to the boron addition, variations of the sizes of these secondary phases were also observed. Although the addition of more boron involved greater formation of precipitates, the proportions between the boron content and the TiB formed were lower at the highest boron content in the starting mixture. The formed TiB and the boron particles significantly contributed to the hardening and stiffness effects. Increasing the temperature helped to increase the stiffness of the composites more than its hardness.

Acknowledgments: The publication has been supported by Junta de Andalucía with project TIC-7528. We thank the Microscopy and the X-Ray Laboratory Services of CITIUS (University of Seville). Furthermore, the authors wish to thank Rayner Simpson for his assistance with the English translation.

Author Contributions: All the authors have been collaborating with each other to obtain a high quality research work. Isabel Montealegre-Meléndez performed the materials selection, analyzed the data and designed the structure of the paper. Cristina Arévalo has been responsible of microstructure characterization for specimens: optical and electron microscopy, and the relation between processing parameters and materials properties. Enrique Ariza has done the mechanical properties and references selection. Eva M. Perez-Soriano has performed the metallographic preparation and the relation between processing parameters and materials properties. Michael Kitzmantel has controlled the fabrication process. Erich Neubauer has optimized the equipment and applications.

Conflicts of Interest: The authors declare no conflict of interest.

References

1. Ravi Chandran, K.S.; Panda, K.B.; Sahay, S.S. TiBw-reinforced Ti composites: Processing, properties, application prospects, and research needs. *JOM*, **2004**, *56(* 5), pp. 42–48, DOI:10.1007/s11837-004-0127-1.
2. Kondoh, K. 16–Titanium metal matrix composites by powder metallurgy (PM) routes. *Titanium Powder Metallurgy*, **2015**, pp. 277–297.
3. Zhang, J. et al. Microstructure and properties of in situ titanium boride (TiB)/titanium (TI) composites. *Mater. Sci. Eng. A*, **2015**, *648*, pp. 158–163, DOI: 10.1016/j.msea.2015.09.067.
4. Munir, K.S. et al. Microstructure and mechanical properties of carbon nanotubes reinforced titanium matrix composites fabricated via spark plasma sintering. *Mater. Sci. Eng. A*, **2017**, *688*, pp. 505–523, DOI: 10.1016/j.msea.2017.02.019.
5. Ozerov, M.N. et al. Brittle-to-ductile transition in a Ti–TiB metal-matrix composite. *Mater. Lett.*, **2017**, *187*, pp. 28-31, DOI: 10.1016/j.matlet.2016.10.060.
6. Jia, L. et al. Microstructural evolution and competitive reaction behavior of Ti-B_4C system under solid-state sintering. *J. Alloys Compd.*, **2016**, *687*, pp. 1004–1011, DOI: 10.1016/j.jallcom.2016.06.280.
7. Popov, V.A. et al. Particulate metal matrix composites development on the basis of in situ synthesis of TiC reinforcing nanoparticles during mechanical alloying. *J. Alloys Compd.*, **2017**, *707*, pp. 365–370, DOI: 10.1016/j.jallcom.2016.10.051.
8. Jiao, Y. et al. Effects of first-scale TiBw on secondary-scale Ti5Si3 characteristics and mechanical properties of in-situ (Ti5Si3+TiBw)/Ti6Al4V composites. *J. Alloys Compd.*, **2017**, *704*, pp. 269–281, DOI: 10.1016/j.jallcom.2017.02.044.
9. Montealegre-Meléndez, I. et al. Study of Titanium Metal Matrix Composites Reinforced by Boron Carbides and Amorphous Boron Particles Produced via Direct Hot Pressing. *Key Eng. Mater.*, **2016**, *704*, pp. 85–93, DOI: 10.4028/www.scientific.net/KEM.704.85.
10. Hu, Y. et al. In-situ ultrafine three-dimensional quasi-continuous network microstructural TiB reinforced titanium matrix composites fabrication using laser engineered net shaping. *Mater. Lett.*, **2017**, *195*, pp. 116-119, DOI: 10.1016/j.matlet.2017.02.112.

11. Oghenevweta, J.E.; Wexler, D.; Calka, A. Sequence of phase evolution during mechanically induced self-propagating reaction synthesis of TiB and TiB_2 via magnetically controlled ball milling of titanium and boron powders. *J. Alloys Compd.*, **2017**, *701*, pp. 380–391, DOI: 10.1016/j.jallcom.2017.01.016.
12. Schmidt, J.; Boehling, M.; Burkhardt, U. Preparation of titanium diboride TiB_2 by spark plasma sintering at slow heating rate. *Sci. Technol. Adv. Mater.*, **2007**, *8*(5), pp. 376–382, DOI: 10.1016/j.stam.2007.06.009.
13. Sabahi Namini, A.; Azadbeh, M.; Shahedi Asl, M. Effect of TiB_2 content on the characteristics of spark plasma sintered Ti–TiBw composites. *Adv. Powder Technol.*, **2017**, *28*(6), pp. 1564–1572, DOI: 10.1016/j.apt.2017.03.028.
14. Liu, B.X. et al. Fracture behaviors and microstructural failure mechanisms of laminated Ti–TiBw/Ti composites. *Mater. Sci. Eng. A*, **2014**, *611*, pp. 290–297, DOI: 10.1016/j.msea.2014.05.089.
15. Arévalo, C. et al. Influence of Sintering Temperature on the Microstructure and Mechanical Properties of In Situ Reinforced Titanium Composites by Inductive Hot Pressing. *Materials*, **2016**, *9*(11), 919, DOI: 10.3390/ma9110919.
16. Montealegre Meléndez, I.; Neubauer, E.; Danninger, H. Consolidation of titanium matrix composites to maximum density by different hot pressing techniques. *Mater. Sci. Eng. A*, **2010**, *527*(16), pp. 4466–4473, DOI: 10.1016/j.msea.2010.03.093.
17. ASM-International, Nondestructive Evaluation and Quality Control, 9th ed. Ohio, United State of America, 1989.
18. Attar, H. et al. Nanoindentation and wear properties of Ti and Ti-TiB composite materials produced by selective laser melting. *Materials Science and Engineering A*, **2017**, *688*, pp. 20-26, DOI: 10.1016/j.msea.2017.01.096.
19. Wang, B. et al. Modification of microstructure and tensile property of TiBw/near-α Ti composites by tailoring TiBw distribution and heat treatment. *Journal of Alloys and Compounds*, **2017**, *690*, pp. 424-430, DOI: 10.1016/j.jallcom.2016.08.138.
20. Lütjering, G. and Williams, J.C. *Titanium*, 2nd ed.; Springer: Berlin, Germany, 2007.
21. Leyends, C. and Peters, M. *Titanium and Titanium alloys. Fundamentals and applications*, 1st ed.; Wiley-VCH Verlag GmbH & Co. KGaA: Weinheim, Germany, 2003.